Accuracy Evaluation of Robotic Tonometry Pulse Sensor System Based on Radial Artery Pulse Wave Simulator

Min-Ho Jun and Young-Min Kim

***Abstract*— In this article, a robotic applanation tonometry pulse sensor system has been developed to easily detect the pulse pressure index (PPI) using a pulse sensor array and reduce the position errors caused by manual operation when measuring the pulsation location of the subject's wrist using a robotic manipulator with automatic localization and pressurization. The amplitude change and shift of the pulse pressure (PP) caused by the unstable measurement angle of the tonometry device with a single sensor were measured and analyzed through an experiment with varying measurement angles. To evaluate the accuracy of the robotic tonometry system, the set PPI of the pulsatile simulator, which repeatedly generates artificial radial artery pulses, was compared with the PPI values estimated by the proposed methods. Accuracy evaluation of the pulse sensor indicates a coefficient of variability for the measured signals of up to 3.2% and a minimum accuracy of 93.7%; however, the PP calculated by a curve-fitting method applied to the measured signals from the array sensor was improved to an average of less than a 1.0% coefficient of variability and 97.9% accuracy. The developed robotic tonometry system represents a contribution to the radial pulse wave research field, which requires more accurate pulse wave analyses and PP measurements.**

***Index Terms*— Array pulse sensor, precise pulse measurement, pulse pressure (PP), radial artery, radial pulse measurement, robotic applanation tonometry.**

I. Introduction

THE pulse wave measurement of the radial artery using tonometry devices has provided meaningful information for predicting cardiovascular risks [1]–[4]. In particular, pulse diagnosis is an important method for identifying a patient's condition or health status in Korean medicine [5]. In recent decades, many studies of Eastern medicine have aimed to objectify, quantify, and automate wrist pulse diagnosis by employing modern sensors [6]–[9]. Recently, the use of pulse wave measurements, such as tonometry, wrist band, and photoplethysmography (PPG), has been increasing in the fields of integrated medicine and Western medicine. In addition, the difference in radial pulse characteristics between primary dysmenorrhea patients and healthy subjects measured using a tonometry pulse wave measurement system was reported [10], and pulse diagnosis was more noticed. Hence, many research groups have been interested in the development of devices that can measure the pulse wave of the radial artery.

Blood pressure is one of the essential vital signals, and cardiovascular diseases and blood pressure have been known to be highly related [11], [12]. Methods for measuring blood pressure can be divided into two major categories: invasive and noninvasive methods. Invasive methods use a catheter to insert a pressure sensor directly into the artery and are often used in the operating room. Noninvasive methods are usually performed using a pressurized cuff on the upper arm, which is called the oscillometric method. The tonometric method is a noninvasive blood pressure measurement method because it is capable of measuring not only blood pressure but also other vascular indices, such as the augmentation index (AIx) [2], [4], [6], pulse wave velocity [13]–[15], and pulse pressure index (PPI) [10], [16], [17]. However, the tonometric method is not widely used because it is difficult to precisely measure both the radial pulse waveform and the pressurizing force from a single sensor and often obtains different results depending on the user's operation ability. Therefore, the precise control of the contact position, applied pressure magnitude, direction, and so on of the tonometry sensor is required for accurately estimating blood pulse pressure (PP). For this purpose, a robotic tonometry pulse sensor system for precise pressurizing control in the radial artery was developed in our study.

The proposed system, which minimizes the measurement error by the automatic measurement of the tonometry system and increases the measurement accuracy of the maximum PP using a pulse sensor array, was developed to analyze the pulse wave of the radial artery using a precise and noninvasive method. We have developed the robotic tonometry pulse sensor system that consisted of six main components. The developed robotic tonometry system was applied to a pulse wave simulator to confirm the importance of a constant angle and the necessity of an array pulse sensor in the pulse wave measurement and to evaluate the measurement accuracy of the set PP. First, the amplitude change and shift of the pulse signal peak depending on the measurement angle were measured experimentally. The error level caused by the unstable

Manuscript received September 9, 2019; revised February 26, 2020; accepted March 3, 2020. Date of publication March 16, 2020; date of current version September 15, 2020. This work was supported by the Korea Institute of Oriental Medicine (KIOM) through the Korean Government under Grant KSN2012110. The review of this article was arranged by Senior Editor Bruno Ando. *(Corresponding author: Young-Min Kim.)*

The authors are with the Future Medicine Division, Korea Institute of Oriental Medicine (KIOM), Deajeon 34054, South Korea (e-mail: irobo77@kiom.re.kr).

Color versions of one or more of the figures in this article are available online at http://ieeexplore.ieee.org.

Digital Object Identifier 10.1109/TIM.2020.2981107

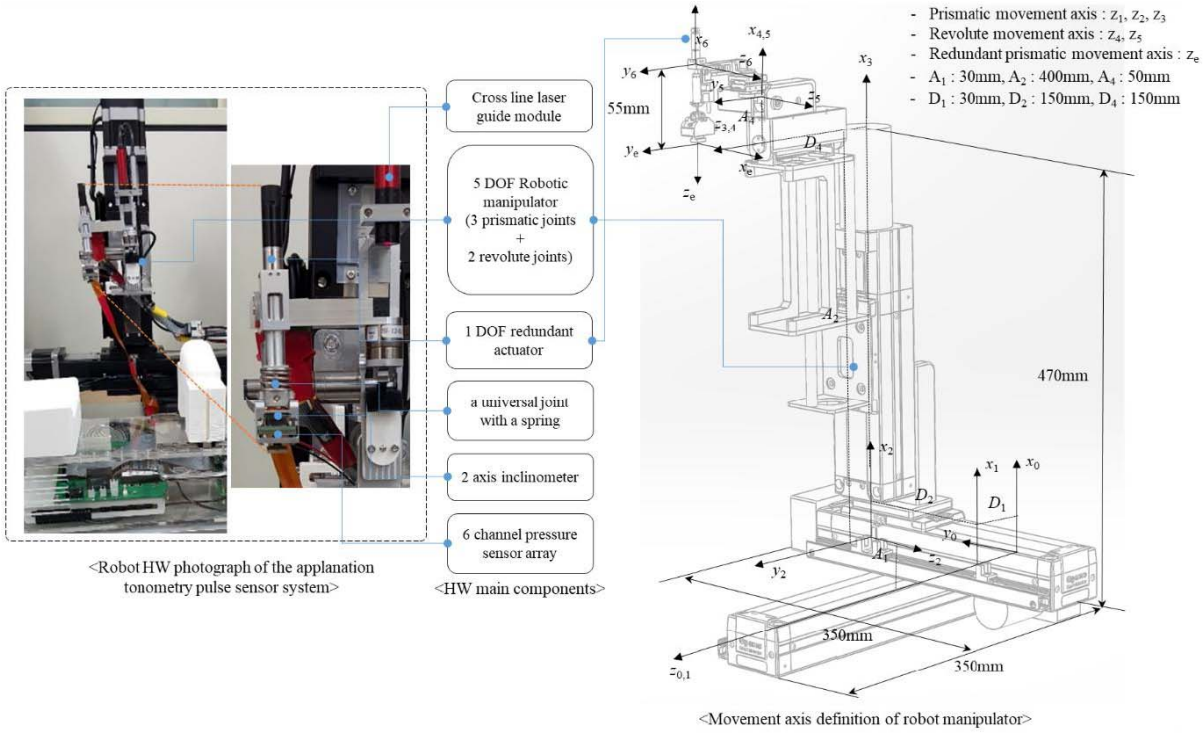

Fig. 1. Main hardware components of a robotic applanation tonometry pulse sensor system and movement axis definitions for robot manipulation.

measurement angle of the tonometry device could be observed from these experiments. In addition, to improve the accuracy of the PP, the maximum pulse amplitude using signals from the pulse sensor array was estimated by the curve-fitting method. The developed tonometry system can be widely used in various applications, such as pulse diagnosis on the radial artery and blood pressure measurements, to achieve precise pulse wave measurements by reducing the measurement errors between users and improving the accuracy due to the use of array sensors.

II. Methods

A. Robotic Tonometry Sensor System

The developed robotic tonometry pulse sensor system consisted of six main components: a cross-line laser, a piezoresistive pulse sensor, a two-axis inclinometer, a spring universal joint, a five-axis robotic manipulator, and a one-axis precision pressure motor, as shown in Fig. 1. Fig. 1 shows the hardware components and configuration of the developed robotic tonometry system and the movement axis definition for robot manipulation. A cross-line laser was used to allow the operator to search for the approximate location of the radial arterial pulsation on the artificial wrist. By coinciding the fingertip of the operator and the center position of the cross line, one can easily mark the approximate location of the radial artery pulse. A piezoresistive pulse sensor used to measure the radial pulse wave was fabricated using an arrangement of six in-line sensor cells (C33, EPCOS, Munich, Germany), and the surface of the pulse sensor was coated with silicone to prevent fracturing of the sensor cells due to contact with the wrist skin [18]. The tilt of the sensor was measured using a two-axis inclinometer (SCA100T-D01, Murata, Manufacture Company, Kyoto, Japan), and the inclinometer was attached integrally to the rear of the pulse sensor. The tilt joint consists of a two-axis universal joint and a spring. The joint is tilted in accordance with the angular changes caused when the pulse sensor is tilted and pressed against the skin layer, and the pulse sensor can move back to its original position when it moves away from the skin. The pulse sensor array, inclinometer, tilt joint, and working mechanism of the spring universal joint are shown in Fig. 2.

The robotic pressure manipulator consists of a five-axis motor system, with three-axis linear translation motion and two-axis rotational motion, so that the pulse sensor can be freely controlled to obtain the pressure angle. In addition, a one-axis motor system with a linear translation motion at the vertical axis of the sensor plane is constructed to achieve stable precise pressure control after the optimal pressure angle is obtained. Finally, a one-axis force sensor (FS2050, TE Connectivity, Fremont, CA, USA) was attached between the manipulator and the precision pressure motor to measure the force applied along the vertical axis. The force sensor was used to measure the force with which the pulse sensor was pressed onto the radial artery to find the start point and the maximum point, at which the pulse wave was at its maximum. In addition, a cross-line laser used to guide the measurement position was installed to reduce the measurement position error of the user, as shown in Fig. 3. Fig. 3(a)–(d) shows the sequence for measuring the pulse wave of the radial artery. The cross-line laser guides the operator to the measurement position with the cross line before measuring the radial artery pulse. When the radial pulse is measured, the robotic tonometry system is automatically moved to the guided position and performs the measurement; this minimizes the error caused by the measurement position, which was a problem in the manual

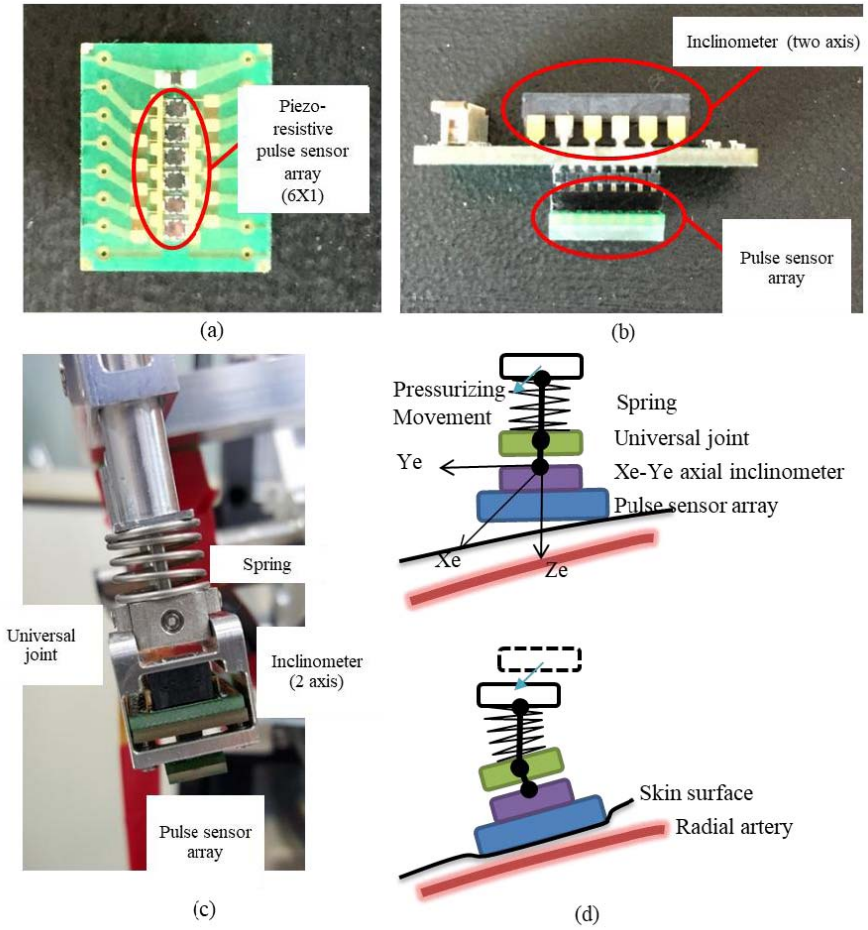

Fig. 2. Structure of the tonometry sensors for the measurement of the radial artery pulse. (a) Array structure of the piezoresistive sensors. (b) Side view of the housing of the tilting sensor and pulse sensor. (c) Sensor mounted on the end-effector of the robot. (d) Working mechanism of the spring universal joint when the sensor comes into contact with the skin after pressurizing movement.

measurement process of a previous tonometry system with a single sensor. Fig. 4 shows the procedures for measuring the radial artery pulse wave and the preprocessing and data acquisition of the measured signals. To measure the radial pulse wave using the developed tonometry system, the operator first finds an approximate location for taking the pulse on the radial artery by the fingertip and places the cross laser at the measurement point. Next, the optimal pressing position and direction are calculated from the signals of the pulse sensor array and the tilting sensor. Finally, the radial artery pulse is measured using a precisely controlled motor with the calculated optimal position and direction. The developed system also automatically adjusts the tilt of the pulse sensor according to the location of the subject's wrist in these radial pulse measuring processes.

B. Experiment on the Robotic Tonometry Pulse Sensor System

To evaluate the performance of the developed robotic tonometry pulse sensor system, experiments were conducted using a compact pulsatile simulator that artificially generated controlled pulse waveforms driven by cams [19]. The reference input signal of the radial pulse waveform generated by the cam-driven simulator was a typical pressure signal from a young adult acquired from clinical data [20]–[22]. In the experiments, the PP values of the simulator were set to 50 and 60 mmHg, and the heart rate (HR) values were 65 and 75 bpm. To precisely and accurately adjust the pressure and HR of the simulator, the pressure and HR were measured from the pressure sensor installed in front of the syringe. The experimental setup for acquiring the pulse signal from the artificial radial artery of the pulsatile simulator is shown in Fig. 5. First, two vertical contact angles were defined for the experiment to determine the maximum PP error for the contact direction of the radial artery, as shown in Fig. 6. The angle α indicates the direction of rotation around the perpendicular axis of the wrist direction, and the angle β indicates the direction of rotation around the axis corresponding to the wrist direction. To investigate the error levels with respect to the measurement angles, the PPI for the rotation angle α was measured at the intervals of 2°–3° from $-3°$ to 12° and the PPI for the rotation angle β was measured at the intervals of 2°–3° from $-10°$ to 6°. The PPI is the PP response upon reaching the maximum pulse amplitude of each pulse signal.

The contact force direction of the pulse sensor could be kept constant when the pulse sensor surface angles with respect to the gravitational axis were controlled by constant target

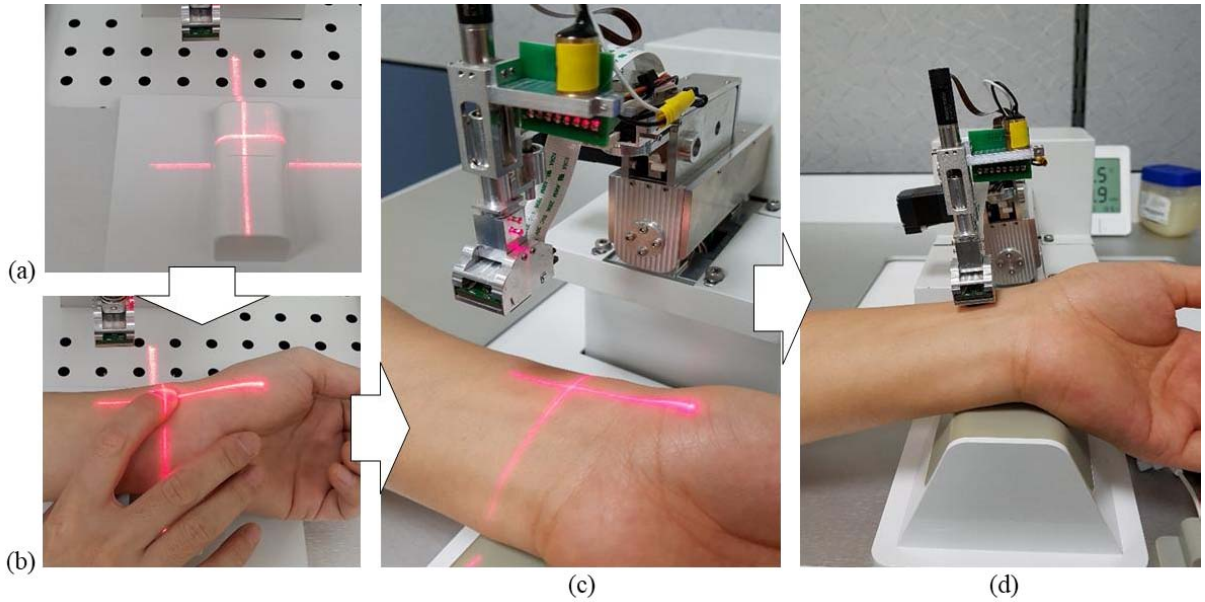

Fig. 3. Image of the cross-line laser used to guide the measurement position installed on the robotic tonometry pulse sensor system. (a) Cross-shaped appearance for guiding the measurement position with the laser before measuring the radial artery pulse. (b) Positioning the laser at the measurement point after detecting the radial artery position using the user's finger. (c) Movement of the pulse sensor to the guided position for measuring the radial artery pulse. (d) Robotic tonometry system that presses the pulse sensor to measure the radial artery pulse at the guided position.

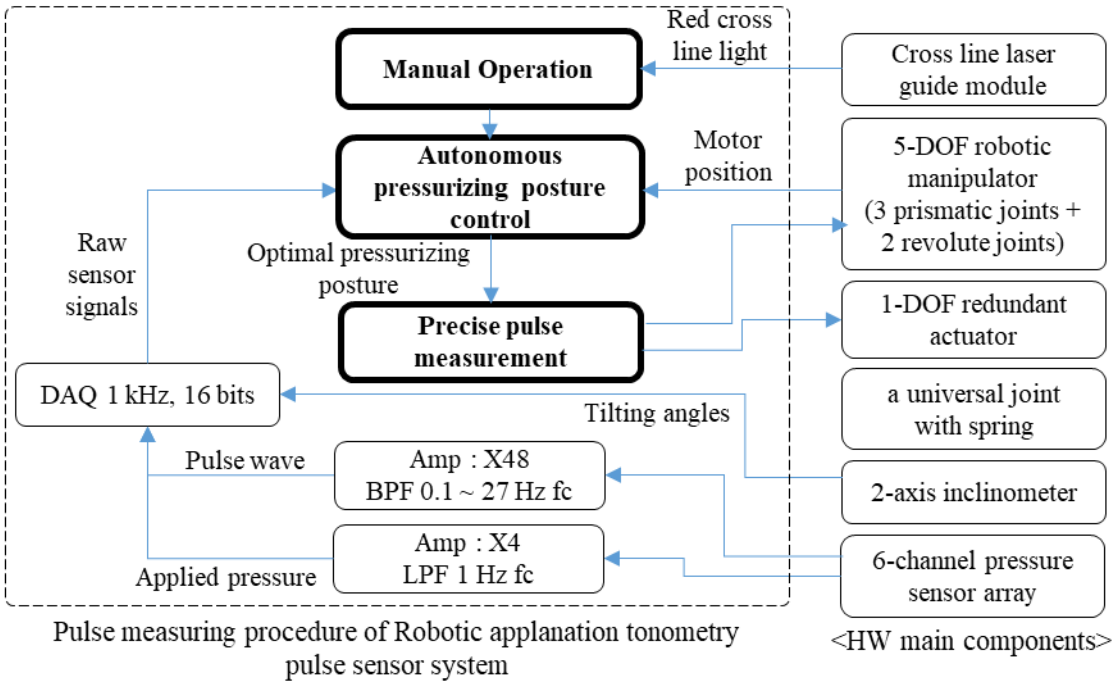

Fig. 4. Radial pulse measurement procedure using the HW components: manual operation—Step 1: the operator searches for the approximate location of the radial artery pulsation on wrist skin using the cross-line laser light. Autonomous pressurizing posture control—Step 2: autonomously calculates the optimal pressurizing positions and directions of the robotic tonometry sensor based on the pulse magnitude values of the pulse sensor array and tilting sensor values. Precise pulse measurement—Step 3: the system transfers the optimal position and direction to the motor target values of the 5-DOF robot manipulator and executes the radial artery pulse measurement by precisely pressurizing the radial artery using a 1-DOF redundant actuator.

values, $\alpha = 6.0°$ and $\beta = -2.0°$, because the artificial arm of the simulator was fixed on the base of the robotic tonometry pulse sensor system. The raw waveform signals generated by the artificial pulsatile simulator were measured using the pressurized pulse sensor from the contact with the artificial wrist surface to the acquisition of the pulse waveform at the maximum PP, as shown in Fig. 7. The center of the pulse sensor was laid on the same contact point of the surface, and the artificial radial artery was incrementally pressed by the pulse sensor until the maximum PP was

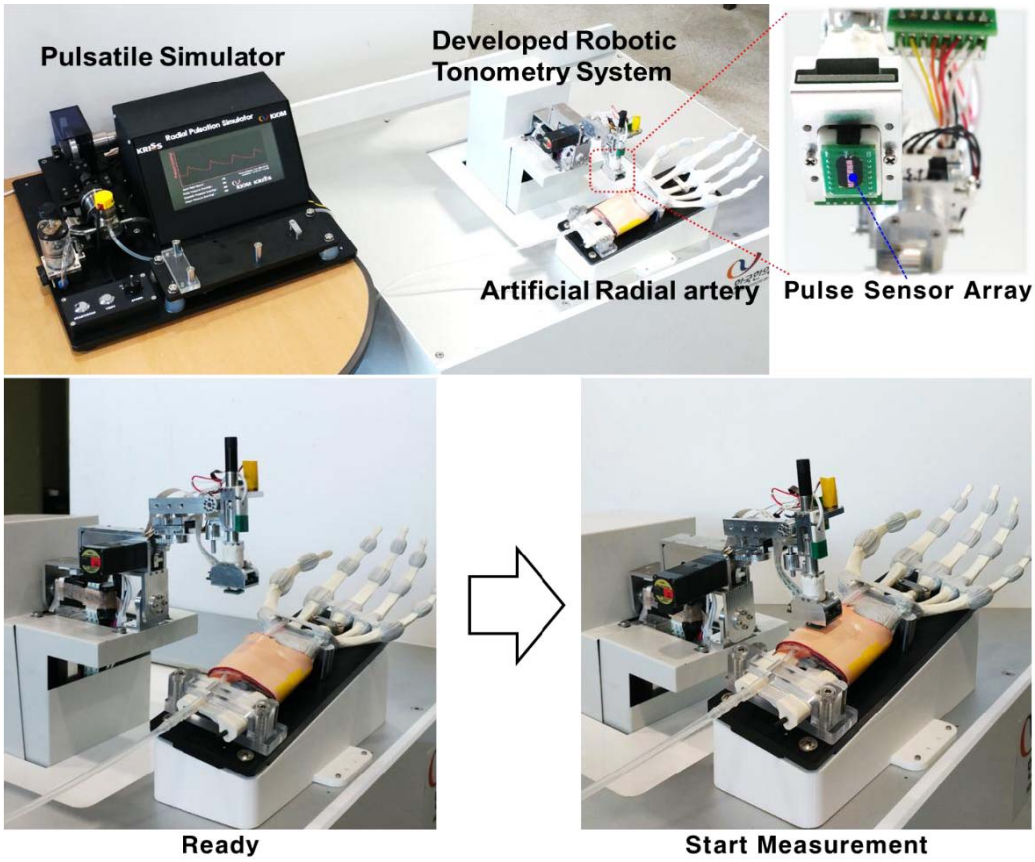

Fig. 5. Experimental setup and measurement for acquiring the pulse signals from the artificial radial artery.

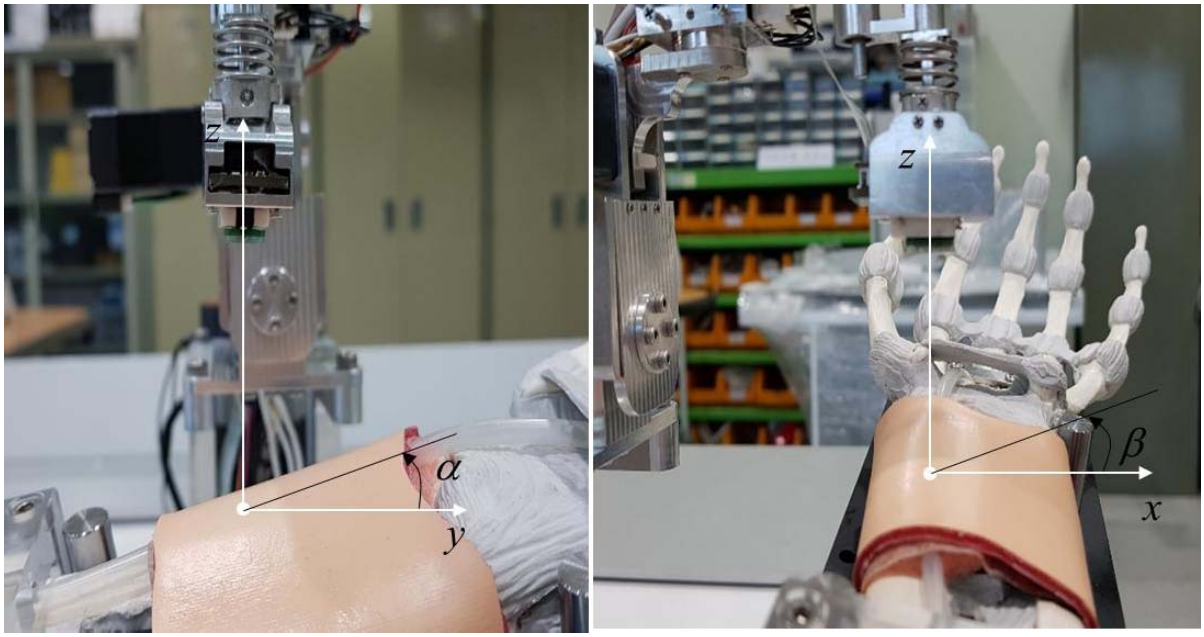

Fig. 6. Representation of the definitions of the two vertical contact angles (α and β) for defining the contact direction with the radial artery.

found. When the maximum PP was detected, the robotic tonometry system maintained the contact force for 30 s to reliably record the raw waveform signals of the artificial radial artery pulse. Approximately 30 pulse waveforms obtained in the reliable region were averaged to analyze the reliability of the robotic tonometry pulse sensor system for different input pulse waves. The signals of the pulse sensor were recorded at a sampling rate of 1000 Hz with a bandpass filter from 0.1 to 27 Hz to remove the ac power noise using a notch filter.

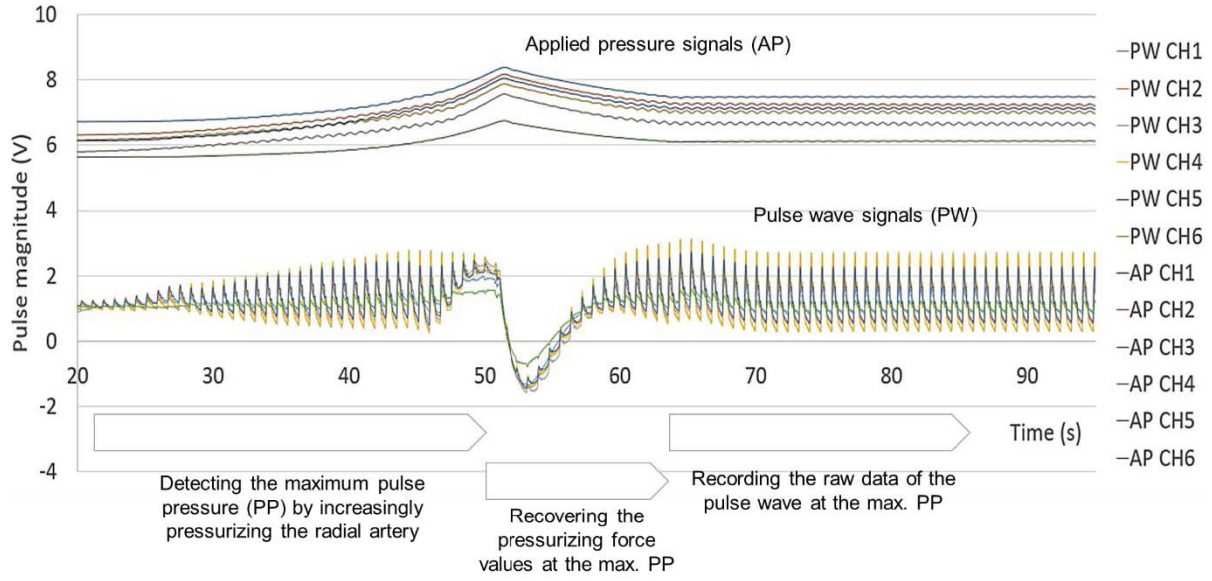

Fig. 7. Raw signals of the artificial pulse wave.

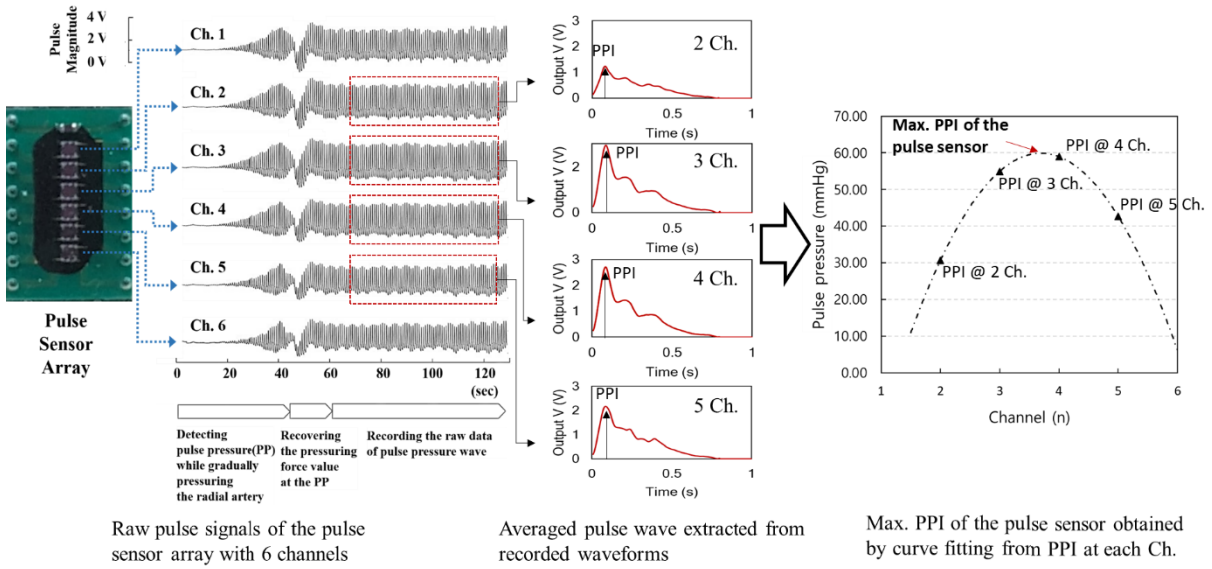

Fig. 8. Signal processing for obtaining the maximum PPI of the pulse sensor from raw pulse signals.

The experiments were conducted to investigate the error level of the measurement angles by setting the artificial pulsatile simulator pressure to 50 mmHg and the HR to 75 bpm. The pulse waves generated by the simulator set at PP values of 50 and 60 mmHg and HRs of 65 and 75 bpm were repeatedly measured three times using the pulse sensor to acquire the raw signals for evaluating the robotic tonometry pulse sensor system. The maximum PP for each channel of the pulse sensor was extracted by the averaged waveforms obtained from the reliable region. The maximum PP of the pulse sensor for the error level was calculated by a quadratic curve-fitting method with the maximum values for each channel of the sensor. The waveforms collected from the four central channels of the pulse sensor, except for the two channels at both ends of the sensor, were used for the second-order polynomial curve-fitting and Gaussian curve-fitting methods to evaluate the accuracy of the robotic tonometry system. The signals for two channels located at the two ends of the pulse sensor were not suitable for analysis due to the noise and difficulty in finding the maximum value. Fig. 8 shows a process for finding the maximum PP of the sensor by curve fitting from the maximum PP at each channel after converting the raw signals acquired by the sensor into the averaged waveform. The values of the maximum PP calculated from the waveforms obtained by three measurements under the same conditions were evaluated to determine the error, and the differences between the maximum values for different PPs and HRs generated by the simulator were compared. In addition, the developed robotic tonometry system was evaluated by comparing the maximum PP values obtained from the curve

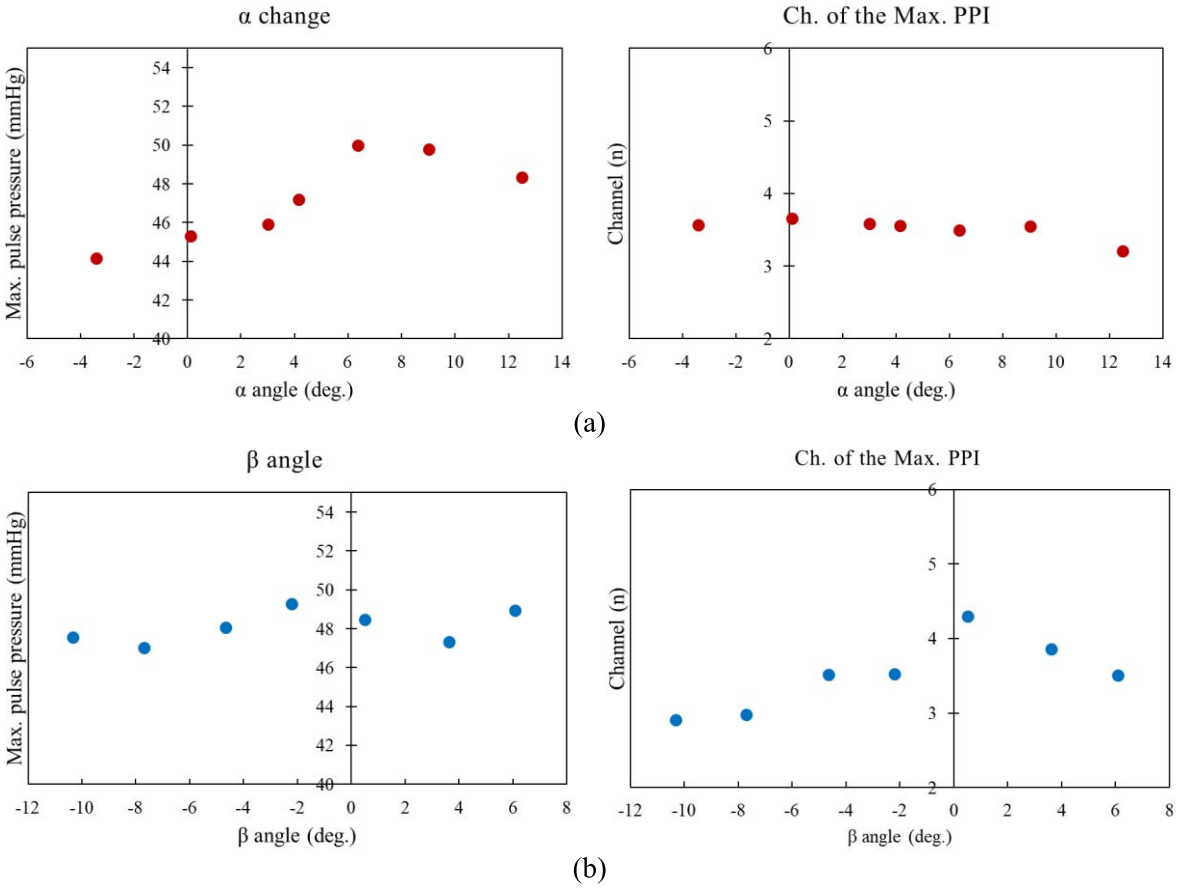

Fig. 9. Error levels and peak channels with respect to the measurement angle. (a) Maximum PPI and peak channel changes with respect to rotation angle α. (b) Maximum PPI and peak channel changes with respect to the rotation angle β.

fitting and the measured signals from the pulse sensor with the PP of the simulator.

III. Results

When the maximum PP was measured while rotating the pulse sensor at an angle α, the maximum PP at 6° was the largest and gradually decreased before 6° and after 6°. Even at the rotation angle of α, the pulse sensor channel with the maximum PP remained between channels 3 and 4. The maximum PP for the rotation angle β was maintained between 47 and 50 mmHg. However, for the rotation angle β, the peak channel was shifted from channels 3 to 4 or higher. Fig. 9 shows the graphs of the maximum PP change due to the rotation angle α and the peak channel shift due to the rotation angle β. Because the artificial radial artery of the pulsatile simulator is initially tilted at an angle α of 6° and an angle β of −2°, the maximum PP was the largest at an angle α of 6°, and the peak pressure was observed between channels 3 and 4 at an angle β of −2°. When the angles are changed from −10° to 6° in the rotation angle β experiment, the peak channel should be moved from channels 3 to 5.

However, it was assumed that the peak channel moved back to channel 3 at an angle β of 0° because channels 5 and 6 of the pulse sensor make the first contact with the skin, and then, the radial artery is slightly shifted. Fig. 10 shows a

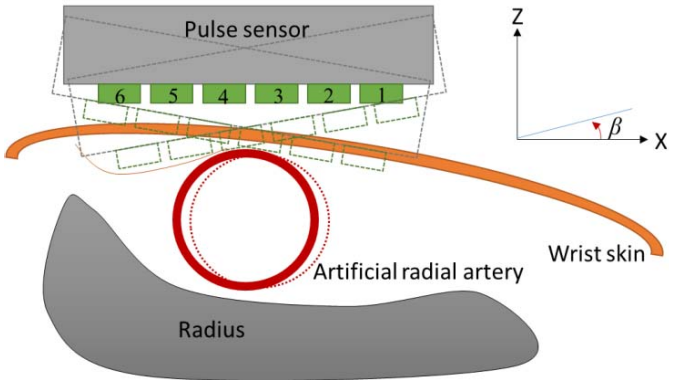

Fig. 10. Schematic of the peak channel change in the rotation angle β experiment.

schematic of the variation in the peak channel in the rotation angle β experiment. Table I shows the results for the α- and β-angle rotation experiments. In the rotation angle α experiment, the difference in the maximum PP was large; however, there was a minimal change in the peak channel. In the rotation angle β experiment, the difference in the maximum PP was small; however, the peak channel was strongly shifted. This indicates that the measurement angle error perpendicular to the wrist direction affects the magnitude of the maximum PP and

TABLE I
DIFFERENCES IN THE MAXIMUM PP AND CHANNEL SHIFT WITH RESPECT TO ROTATION ANGLES α AND β

Rotation	Difference of Max. PPI. (mmHg)	Shift of Ch. (n)
α angles	5.84 (11.68 %)	0.46
β angles	2.24 (4.48 %)	1.39

Max. PP.: the maximum pulse pressure, Ch.: channel of the pulse sensor

TABLE II
RATIO AND MEAN OF THE MAXIMUM PPI VALUES OBTAINED USING THE MEASURED PULSE SENSOR AND THE CURVE-FITTING TO THE SET PRESSURE OF THE PULSATILE SIMULATOR

Condition	Accuracy (%)			CV (%)		
	Max. Ch.	2-polynomial	Gaussian	Max. Ch.	2-polynomial	Gaussian
HR 75/PP 60	97.75	98.10	99.11	0.43	1.32	1.22
HR 65/PP 60	93.68	95.49	95.29	1.13	0.97	0.97
HR 75/PP 50	97.20	98.38	96.31	2.19	1.32	1.71
HR 65/PP 50	97.06	99.58	97.41	3.24	0.21	2.37
Avg. (%)	96.42	97.89	97.03	1.75	0.95	1.57

CV is the coefficient of variation, Max. Ch. is the ratio of the maximum measured value obtained by the pulse sensor to the set pressure value of the simulator as a percentage, 2- polynomial is the ratio of the maximum value derived by curve-fitting of the 2nd-order polynomial function as a percentage, Gaussian is the ratio of the maximum value derived by curve-fitting with the Gaussian function as a percentage, HR 75/PP 60 represents the set values of the simulator with an HR of 75 bpm and PP of 60 mmHg, HR 65/PP 60 means an HR of 65 bmp and PP of 60 mmHg, HR 75/PP50 means an HR of 75 bpm and PP of 50 mmHg, HR 65/PP50 means an HR of 65 bpm and PP of 50 mmHg, and Avg. is the average value for each column.

that the measurement angle error of the axis corresponding to the wrist direction affects the peak channel shift. Therefore, a measurement system with a constant angle and array pulse sensor can achieve reduced measurement error compared to a tonometry measurement system with a single sensor.

Fig. 11 shows the curve-fitting results for the second-order polynomial function and Gaussian function of different HRs and PPs for pulse waveform signals obtained by the pulse sensor. The markers (■, ●, and ▲) represent the magnitude of the maximum PP of each channel for three trials, and the curve-fitting results calculated from the markers are indicated by lines (—, - - -, and -·-·-). Curve fitting with a Gaussian function has been used in previous studies to find the maximum peak of the waveform measured in the radial artery [23], [24]. The maximum values of the measured pulse sensor signals, the second-order polynomial curve fitting, the Gaussian curve fitting, and the settings of the pulsatile simulator were compared. For the two experiments in which Gaussian curve fitting did not apply, sinusoidal curve fitting was applied to find the maximum PP. The ratio of the maximum PP values as percentages obtained by the measurement and curve fitting to the set pressure of the pulsatile simulator is summarized in Table II. The accuracy is calculated as follows:

$$A_{\mathrm{PP}}(\%) = \frac{\mathrm{PP}_0 - |(\mathrm{PP}_0 - \mathrm{PP}_i)|}{\mathrm{PP}_0} \times 100 \qquad (1)$$

where A_{PP} is the accuracy of the maximum PP, PP_0 is the set PP of the simulator, and PP_i is the measured or calculated maximum PP. The average of the maximum PP values measured using the pulse sensor was 96.42% of the set pressure of the simulator, the calculated value from curve fitting using a second-order polynomial was 97.89%, and the calculated value of the Gaussian curve fitting was 97.03%. Obviously, the maximum PP values derived by the curve-fitting methods were closer to the settings of the simulator than those of the array pulse sensor. In addition, the maximum PP values derived by the second-order polynomial curve fitting were closer to the settings of the simulator than those derived by the Gaussian curve-fitting. In the coefficient of variation (CV) results, the second-order polynomial curve fitting showed the smallest variability in this experiment. This indicates that finding the maximum PP using the second-order polynomial curve-fitting method for pulse signals obtained using the array pulse sensor can increase the accuracy and precision of determining the PP. There were minimal fluctuations in the PP because the change in the HR did not greatly affect the pulse sensor signals.

IV. DISCUSSION

It is important to find the location of the maximum PP on the radial artery because it is difficult to locate the radial artery

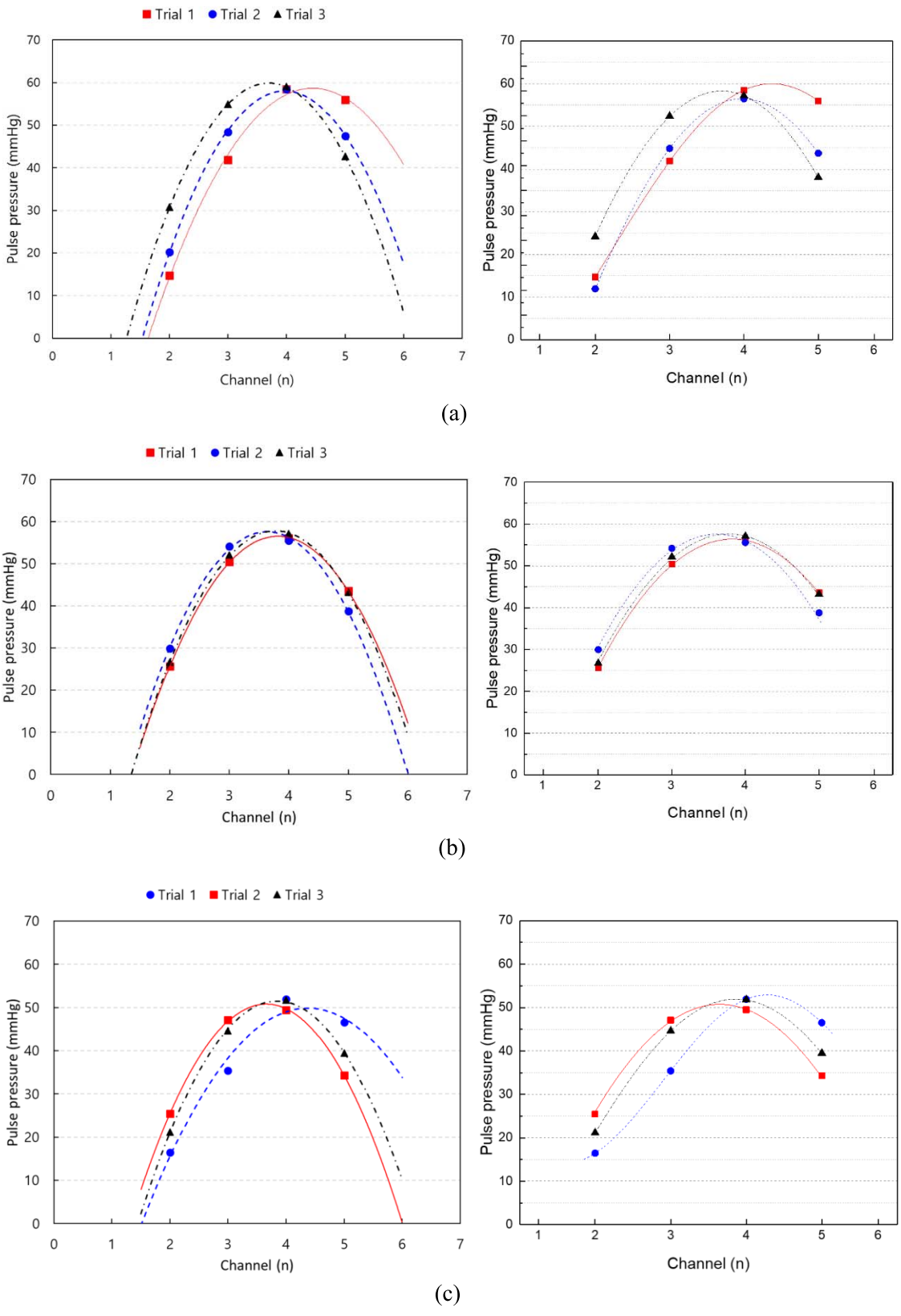

Fig. 11. Maximum PPI values (■, ●, and ▲) at each pulse sensor channel and curve-fitting results for a second-order polynomial function (left lines) and a Gaussian function (right lines) of different HRs and PPs for three trials. (a) Curve-fitting results for a second-order polynomial function and a Gaussian function of the HR 75 and PP 60 pulse waveforms. (b) Curve-fitting results for a second-order polynomial function and Gaussian function of the HR 65 and PP 60 pulse waveforms. (c) Curve-fitting results for a second-order polynomial function and Gaussian function of the HR 75 and PP 50 pulse waveforms. (d) Curve-fitting results for a second-order polynomial function and Gaussian function of the HR 65 and PP 50 pulse waveforms.

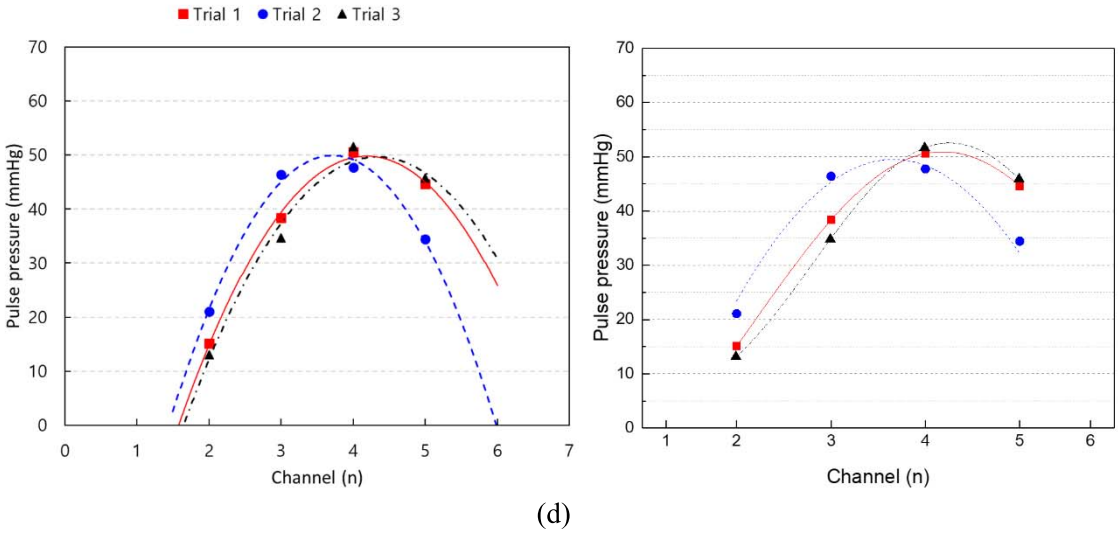

Fig. 11. *(Continued.)* Maximum PPI values (■, ●, and ▲) at each pulse sensor channel and curve-fitting results for a second-order polynomial function (left lines) and a Gaussian function (right lines) of different HRs and PPs for three trials. (a) Curve-fitting results for a second-order polynomial function and a Gaussian function of the HR 75 and PP 60 pulse waveforms. (b) Curve-fitting results for a second-order polynomial function and Gaussian function of the HR 65 and PP 60 pulse waveforms. (c) Curve-fitting results for a second-order polynomial function and Gaussian function of the HR 75 and PP 50 pulse waveforms. (d) Curve-fitting results for a second-order polynomial function and Gaussian function of the HR 65 and PP 50 pulse waveforms.

under the skin. In-line array pressure sensors are better alternatives to single tonometry sensors for conveniently obtaining the position of the maximum PP. Many types of pulse sensor arrays have been used in numerous studies to measure radial artery pulse waves. Hu *et al.* [25] used a capacitive array sensor with 12 sensing points to determine the optimal pulse-taking position. Peng and Lu [26] introduced a flexible 5 × 5 capacitive pressure sensor array for determining pulse patterns. Jun *et al.* [7] used a circular array sensor with seven independent pressure sensors to estimate the direction of the radial artery and reported a study on the development of a seven-channel pulse sensor array [18]. These studies emphasize the importance of locating the maximum pulse amplitude on the radial artery. Therefore, accurately measuring the maximum PPI can improve the repeatability and reliability of radial PP measurements. In our experiments, it was difficult to accurately measure the PP due to changes in the pulse amplitude or peak channel depending on the contact angle between the pulse sensor array and the wrist skin. Therefore, a pulse measurement system has been developed to improve the accuracy of the PP measurement by simultaneously easily marking the measurement position with a cross-line laser, constantly adjusting the contact angle using a robotic manipulation system, and locating the maximum PP with a pulse sensor array.

Methods for finding or estimating the maximum PPI on the radial artery using various fitting methods of the pulse signals collected using array pulse sensors have not been extensively studied. It is also unclear which methods for estimating the maximum PP of the radial artery wave measured noninvasively are the most appropriate. We have only shown in our experiments that the second-order polynomial curve-fitting method was more appropriate for estimating the maximum PP than the Gaussian curve-fitting method. Therefore, further studies on optimized curve-fitting methods are needed to find the maximum PP from the measured signals of the array pulse sensor.

Conventional tonometry systems with a single sensor have shown that it is difficult to make accurate measurements with various parameters, such as the measurement position, applied pressure, and measurement angle, because the operators need high-level training to subtly control the measurement parameters. However, there are few studies on the range of errors occurring when the radial artery pulse is measured using a tonometry device with a sensor. Therefore, to confirm the accuracy improvement achieved by reducing the user's positioning error, quantitative studies on the error of pulse wave measurements due to the manual control of conventional tonometry devices are needed. In addition, the peak channel should be gradually moved toward the direction of rotation in the β angle experiment; however, it was assumed that the peak channel moving back to the center is due to the shift of the artificial radial artery. This result may be different in human body studies, and much research is needed on the shift of the peak channel under rotations by an angle β.

We used the controllable pulsatile simulator to set the reference values of the PP and HR; however, they may be different from the characteristics of the radial artery pulse wave in the human body. Because the developed robotic tonometry system is intended to measure the pulse wave and blood pressure on the radial artery in the human body, the accuracy of the developed system should be evaluated after conducting clinical trial studies. In addition, it is necessary to develop algorithms for locating a suitable measurement position of the pulse sensor to measure the radial artery pulse in the human body because the position and shape of each subject's wrist are different.

The precise measurement of the radial pulse wave should be a priority for the accurate assessment of the

blood pressure (BP), augmentation index (AIx), and pulse wave velocity (PWV), which are used to examine health conditions in the clinic. In the reproducibility of previous commercial devices, a hand-held tonometer (SPT-301, Millar Instruments, Houston, TX, USA) showed a mean difference of 0.033 in AIx after two repeated measurements [27]. It has been reported that AIx values of other arterial applanation tonometry devices (SphygmoCor, Atcor-Medical, Sydney, Australia) had a standard deviation (SD) of 3%–8% for intervisit reproducibility [28]–[30]. In a comparison of BP between an A-line (catheter) and a radial tonometry device (TL-200 or TL-200pro; Tensys Medical, Inc., San Diego, CA, USA), the mean differences within 10% were 79% in systolic BP, 63% in diastolic BP, and 52% in mean BP [31]. In addition, it has been reported that the mean difference between two operators could be up to 9% in AIx with radial tonometry devices (SphygmoCor, Atcor-Medical, Sydney, Australia) [32]. In comparison to the results of the developed system and commercial devices, the average AIx mean difference for the developed system was 0.005 for the 12 measurements, which is approximately 1/6 of that of the commercial devices in the literature. In addition, the CV, which shows the measurement precision (repeatability) for the developed system, was 0.8% for AIx and 1.7% for PP. These results indicate that the developed system has much better precision than the existing devices, given that the CV of the commercial devices was approximately 5%–8% through experiments of the above-cited articles. Although the precision test results of the developed system were obtained using a pulsation simulator, there is a sufficient possibility to estimate accurate BP and AIx values through future clinical trials.

V. Conclusion

A robotic applanation tonometry pulse sensor system that can easily detect the maximum PP using array pulse sensors and reduce the position errors caused by the user's manual control of the measurement position on the subject's wrist by applying a cross-line laser and robotic manipulator with automatic localization and pressurization has been developed. The developed robotic tonometry system was applied to a pulse wave simulator to confirm the importance of a constant angle and the necessity of an array pulse sensor for the pulse wave measurement and to evaluate the measurement accuracy of the set PP. The amplitude and shift of the PP peaks caused by the unstable measurement angle of the tonometry device with a single sensor were measured and analyzed through an experiment with varying measurement angles. To evaluate the accuracy of the robotic tonometry system, the set PP of the pulsatile simulator was compared with the values measured using the pulse sensor and calculated by curve-fitting methods. The accuracy evaluation of the pulse sensor showed a coefficient of variability for the measured signals up to 3.2% and a minimum accuracy of 93.7%. However, the PP calculated by the curve-fitting method applied to the measured signals from the array sensor was improved, with an average coefficient of variability of less than 1.0% and an accuracy of 97.9%. The developed robotic tonometry system represents a contribution to the radial pulse wave research field, which requires more accurate pulse wave and PP measurements.

References

[1] W. Nichols, "Clinical measurement of arterial stiffness obtained from noninvasive pressure waveforms," *Amer. J. Hypertension*, vol. 18, pp. 3–10, Jan. 2005.

[2] K. Kohara, Y. Tabara, A. Oshiumi, Y. Miyawaki, T. Kobayashi, and T. Miki, "Radial augmentation index: A useful and easily obtainable parameter for vascular aging," *Amer. J. Hypertension*, vol. 18, no. 1, pp. 11s–14s, Jan. 2005.

[3] J. L. Ramirez *et al.*, "Radial artery tonometry is associated with major adverse cardiac events in patients with peripheral artery disease," *J. Surgical Res.*, vol. 235, pp. 250–257, Mar. 2019.

[4] N. Watanabe *et al.*, "Use of the augmentation index from applanation tonometry of the radial artery for assessing the extent of coronary artery calcium as assessed by coronary computed tomography," *Clin. Experim. Hypertension*, vol. 39, no. 4, pp. 355–360, May 2017.

[5] H. Kim, J. Y. Kim, Y.-J. Park, and Y.-B. Park, "Development of pulse diagnostic devices in Korea," *Integrative Med. Res.*, vol. 2, no. 1, pp. 7–17, Mar. 2013, doi: 10.1016/j.imr.2013.01.003.

[6] J.-Z. Wang *et al.*, "A new tonometric device for radial augmentation index and subendocardial viability ratio: Potential use in health screening," *J. Clin. Hypertension*, vol. 16, no. 10, pp. 707–712, Oct. 2014, doi: 10.1111/jch.12396.

[7] M.-H. Jun, Y.-M. Kim, J.-H. Bae, C. Jung, J.-H. Cho, and Y. Jeon, "Development of a tonometric sensor with a decoupled circular array for precisely measuring radial artery pulse," *Sensors*, vol. 16, no. 6, p. 768, 2016.

[8] D. Wang, D. Zhang, and G. Lu, "A novel multichannel wrist pulse system with different sensor arrays," *IEEE Trans. Instrum. Meas.*, vol. 64, no. 7, pp. 2020–2034, Jul. 2015.

[9] R. Velik, "An objective review of the technological developments for radial pulse diagnosis in traditional Chinese medicine," *Eur. J. Integrative Med.*, vol. 7, no. 4, pp. 321–331, Aug. 2015.

[10] J. Kim *et al.*, "A comparative study of the radial pulse between primary dysmenorrhea patients and healthy subjects during the menstrual phase," *Sci. Rep.*, vol. 9, no. 1, pp. 1–11, Dec. 2019.

[11] N. H. Cho *et al.*, "Effect of blood pressure on cardiovascular diseases at 10-year follow-up," *Amer. J. Cardiol.*, vol. 123, no. 10, pp. 1654–1659, May 2019, doi: 10.1016/j.amjcard.2019.02.026.

[12] E. Rapsomaniki *et al.*, "Blood pressure and incidence of twelve cardiovascular diseases: Lifetime risks, healthy life-years lost, and age-specific associations in 1·25 million people," *Lancet*, vol. 383, no. 9932, pp. 1899–1911, May 31, 2014, doi: 10.1016/S0140-6736(14)60685-1.

[13] L.-J. Qiao *et al.*, "The association of radial artery pulse wave variables with the pulse wave velocity and echocardiographic parameters in hypertension," *Evidence-Based Complementary Alternative Med.*, vol. 2018, Dec. 2018, Art. no. 5291759, doi: 10.1155/2018/5291759.

[14] H. Kamran *et al.*, "Comparison of hyperemic changes in carotid-radial pulse wave velocity by upper and lower arm cuff occlusion," *Angiology*, vol. 62, no. 5, pp. 409–414, Jul. 2011, doi: 10.1177/0003319710389022.

[15] A. S. Ferreira, M. A. R. Santos, J. B. Filho, I. Cordovil, and M. N. Souza, "Determination of radial artery compliance can increase the diagnostic power of pulse wave velocity measurement," *Physiolog. Meas.*, vol. 25, no. 1, pp. 37–50, Feb. 2004.

[16] B. J. Lee, Y. J. Jeon, J.-H. Bae, M. H. Yim, and J. Y. Kim, "Gender differences in arterial pulse wave and anatomical properties in healthy Korean adults," *Eur. J. Integrative Med.*, vol. 25, pp. 41–48, Jan. 2019.

[17] B. J. Lee, Y. J. Jeon, B. Ku, J. U. Kim, J.-H. Bae, and J. Y. Kim, "Association of hypertension with physical factors of wrist pulse waves using a computational approach: A pilot study," *BMC Complementary Alternative Med.*, vol. 15, no. 1, p. 222, Jul. 2015.

[18] M.-H. Jun, Y. J. Jeon, J.-H. Cho, and Y.-M. Kim, "Pulse wave response characteristics for thickness and hardness of the cover layer in pulse sensors to measure radial artery pulse," *Biomed. Eng. OnLine*, vol. 17, no. 1, pp. 1–15, Sep. 2018.

[19] T.-H. Yang, G. Jo, J.-H. Koo, S.-Y. Woo, J. U. Kim, and Y.-M. Kim, "A compact pulsatile simulator based on cam-follower mechanism for generating radial pulse waveforms," *Biomed. Eng. OnLine*, vol. 18, no. 1, p. 1, Dec. 2019, doi: 10.1186/s12938-018-0620-3.

[20] T.-H. Kim *et al.*, "Hemodynamic changes caused by acupuncture in healthy volunteers: A prospective, single-arm exploratory clinical study," *BMC Complementary Alternative Med.*, vol. 17, no. 1, p. 274, May 2017, doi: 10.1186/s12906-017-1787-z.

[21] J. H. Bae *et al.*, "Radial pulse and electrocardiography modulation by mild thermal stresses applied to feet: An exploratory study with randomized, crossover design," *Chin. J. Integrative Med.*, Nov. 2017, doi: 10.1007/s11655-017-2972-0.
[22] J.-H. Bae, Y. J. Jeon, S. Lee, and J. U. Kim, "A feasibility study on age-related factors of wrist pulse using principal component analysis," in *Proc. 38th Annu. Int. Conf. IEEE Eng. Med. Biol. Soc. (EMBC)*, Aug. 2016, pp. 6202–6205, doi: 10.1109/EMBC.2016.7592145.
[23] C.-C. Tyan, S.-H. Liu, J.-Y. Chen, J.-J. Chen, and W.-M. Liang, "A novel noninvasive measurement technique for analyzing the pressure pulse waveform of the radial artery," *IEEE Trans. Biomed. Eng.*, vol. 55, no. 1, pp. 288–297, Jan. 2008, doi: 10.1109/TBME.2007.910681.
[24] S.-H. Liu and C.-C. Tyan, "Quantitative analysis of sensor for pressure waveform measurement," *Biomed. Eng. OnLine*, vol. 9, no. 1, p. 6, Jan. 2010, doi: 10.1186/1475-925X-9-6.
[25] C.-S. Hu, Y.-F. Chung, C.-C. Yeh, and C.-H. Luo, "Temporal and spatial properties of arterial pulsation measurement using pressure sensor array," *Evidence-Based Complementary Alternative Med.*, vol. 2012, pp. 1–9, Jun. 2012.
[26] J.-Y. Peng and M. S.-C. Lu, "A flexible capacitive tactile sensor array with CMOS readout circuits for pulse diagnosis," *IEEE Sensors J.*, vol. 15, no. 2, pp. 1170–1177, Feb. 2015.
[27] O. Vardoulis *et al.*, "*In vivo* evaluation of a novel, wrist-mounted arterial pressure sensing device versus the traditional hand-held tonometer," *Med. Eng. Phys.*, vol. 38, no. 10, pp. 1063–1069, Oct. 2016.
[28] C. F. Clarenbach *et al.*, "Comparison of photoplethysmographic and arterial tonometry-derived indices of arterial stiffness," *Hypertension Res.*, vol. 35, no. 2, pp. 228–233, Feb. 2012.
[29] M.-H. Hwang *et al.*, "Validity and reliability of aortic pulse wave velocity and augmentation index determined by the new cuff-based SphygmoCor Xcel," *J. Hum. Hypertension*, vol. 28, no. 8, pp. 475–481, Aug. 2014.
[30] A. Lowenthal *et al.*, "Arterial applanation tonometry: Feasibility and reproducibility in children and adolescents," *Amer. J. Hypertension*, vol. 27, no. 9, pp. 1218–1224, Sep. 2014.
[31] R. Dueck, O. Goedje, and P. Clopton, "Noninvasive continuous beat-to-beat radial artery pressure via TL-200 applanation tonometry," *J. Clin. Monitor. Comput.*, vol. 26, no. 2, pp. 75–83, Apr. 2012.
[32] M. Crilly, C. Coch, M. Bruce, H. Clark, and D. Williams, "Indices of cardiovascular function derived from peripheral pulse wave analysis using radial applanation tonometry: A measurement repeatability study," *Vascular Med.*, vol. 12, no. 3, pp. 189–197, Aug. 2007.

Min-Ho Jun received the B.S. degree in mechanical engineering from Chungnam National University, Daejeon, South Korea, in 2004, and the M.S. and Ph.D. degrees in mechatronics engineering from the Gwangju Institute of Science and Technology (GIST), Gwangju, South Korea, in 2007 and 2014, respectively.

Since 2014, he has been a Researcher with the Korea Institute of Oriental Medicine (KIOM), Deajeon. His research interests include the development of medical devices for Korean medicine, wearable sensors for health monitoring, bio-signal measurement and analysis, medical MEMS devices, and medical applications for healthcare.

Young-Min Kim received the B.S. degree in mechanical engineering from Yonsei University, Seoul, South Korea, in 1999, the M.S. degree in mechanical engineering from the Pohang University of Science and Technology (POSTECH), Pohang, South Korea, in 2001, and the Ph.D. degree in mechanical engineering from the Korea Advanced Institute of Science and Technology (KAIST), Deajeon, South Korea, in 2011.

From 2002 to 2006, he was a Research Scientist with the Human-Welfare Robotic System Research Center, KAIST. Since 2011, he has been a Principle Researcher with the Future Medicine Division, Korea Institute of Oriental Medicine, Deajeon. His research interests include the medical devices for the personalized healthcare, wearable sensors for daily health monitoring, sophisticated human–robot interface (HRI) technology, and innovative HRI applications.